Journal of Natural Gas Science and Engineering 10 (2013) 8–13

Contents lists available at SciVerse ScienceDirect

Journal of Natural Gas Science and Engineering

journal homepage: www.elsevier.com/locate/jngse

Active constraint regions for a natural gas liquefaction process

Magnus G. Jacobsen [a], Sigurd Skogestad [b,*]

[a] ABB AS, 0666 Oslo, Norway
[b] Department of Chemical Engineering, Norwegian University of Science and Technology, 7491 Trondheim, Norway

ARTICLE INFO

Article history:
Received 5 August 2011
Received in revised form
30 August 2012
Accepted 16 October 2012
Available online 26 November 2012

Keywords:
Self-optimizing control
Liquefied natural gas
LNG
PRICO
Disturbances
Optimal operation

ABSTRACT

Optimal operation of liquefaction processes is little studied in the open literature. In particular, the issue of how optimal operation changes with disturbances has received very little attention. This paper addresses optimal operation of a simple natural gas liquefaction process – the PRICO process. The focus is on how the active process constraints change with disturbances. It is shown that the feasible part of the disturbance space can be divided into five regions with different sets of active constraints. We also suggest control structures for the process, and find that as little as two control structures may be needed despite of the fact that there are five regions. It is suggested to use compressor speed to control the margin to surge at minimum, and to keep the turbine outlet stream at saturation at all times.

1. Introduction

Liquefaction of natural gas is an energy-intensive process, and efficient operation typically means great savings. One of the most important aspects in optimal operation is to control the active constraints. However, little literature exists on optimal operation, active constraints and selection of controlled variables. Papers addressing optimal operation of LNG processes include Lee et al. (2002), Pillarella et al. (2005), Jensen and Skogestad (2006), and Nogal et al. (2008). Selection of controlled variables was addressed by Singh et al. (2008) and Michelsen et al. (2010).

In our earlier paper (Jacobsen and Skogestad, 2011a), we studied how active constraints for optimal operation varied with disturbances, for different processes. Knowledge of this is very useful when designing the control structure of a plant, because one has to control the active constraints to have optimal operation. Here, we apply the experiences from those two papers to map active constraint regions for a natural gas liquefaction process.

We have chosen to study the PRICO process (Price and Mortko, 1996), which is the one used by Jensen and Skogestad (2006). The PRICO process is chosen because it is simple, while still capturing the fundamental issues one will also find in more complex liquefaction processes.

2. Optimal operation of a PRICO liquefaction plant

2.1. Plant description

The PRICO process (Price and Mortko, 1996) (Fig. 1) is a very simple liquefaction process. The natural gas feed stream (NG IN) enters from the left, and is liquefied and subcooled to −157 °C in the heat exchanger. It is then expanded (not shown here) and pumped to a storage tank. The mixed refrigerant (MR) is condensed with sea water or air (MR-3), before it is liquefied in the heat exchanger (MR-4). It is then expanded to a lower pressure, giving a lower temperature (MR-5, MR-6), before it is used for cooling in the heat exchanger. It leaves the heat exchanger in a superheated state (MR-1) and is compressed back to high pressure (MR-2). The heat exchanger is typically a plate-and-fin type heat exchanger.

2.2. Model and simulation tools

We have used Honeywell Unisim for modelling the process. For optimization, we have used MATLAB. The two are linked through the COM interface. We have used stream data from the nominal optimum reported in Jensen and Skogestad (2006), the compressor curves are also copied from that paper. The combination of Unisim for modelling and MATLAB for optimization was also used by Aspelund et al. (2010), but they used a Tabu search algorithm (Chelouah and Siarry, 2005) whereas we use MATLAB's built-in **fmincon** solver. The stream variables we have copied are

* Corresponding author. Tel.: +47 735 94154.
E-mail address: skoge@chemeng.ntnu.no (S. Skogestad).

1875-5100/$ – see front matter © 2012 Elsevier B.V. All rights reserved.
http://dx.doi.org/10.1016/j.jngse.2012.10.002

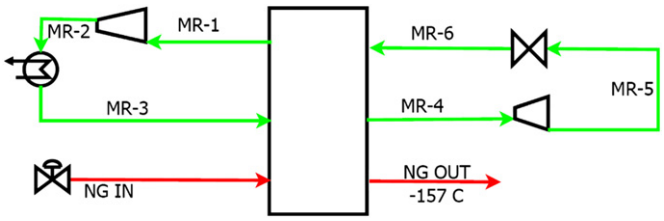

Fig. 1. Simplified flowsheet of the PRICO process as modelled by Jensen and Skogestad (2006), not including expansion of cold natural gas.

summarized in Table 1. Due to a slightly different heat exchanger model, and to the fact that gPROMS and Unisim use different sources for the parameters used in the SRK equation of state, there are small differences in some other key variables. These are summarized in Table 2.

As described in Jacobsen and Skogestad (2011b), the three-stream heat exchanger model has been solved by adding two temperatures to the specification vector, and adding the heat exchanger *UA* specifications to the optimization problem as equality constraints. In addition, we needed to tear the compressor inlet stream, because the use of compressor curves demands that the inlet conditions of the compressor are fully specified. The temperature of the torn stream is added to the decision variables, and convergence of the torn stream is included as a third equality constraint. Thus the optimization problem includes three equality constraints:

$$\begin{aligned} UA_1 &= UA_{1,\text{specified}} \\ UA_2 &= UA_{2,\text{specified}} \\ T_{\text{MR-1,calculated}} &= T_{\text{MR-1,guessed}} \end{aligned} \tag{1}$$

2.3. Optimization objective

In the PRICO process, there is one product stream and two utilities that are used (power for compression, and for pumping of cooling water). It is reasonable to ignore the cost of pumping cooling water, since this is very small compared to the power consumed by the compressor.[1] When the cost of cooling water is ignored, the objective function to be minimized (with units \$/s) can be expressed as follows:

$$J = p_{\text{work}} \cdot W_s - p_{\text{LNG}} \cdot F_{\text{LNG}} \tag{2}$$

where p_{work} is the price of energy (in \$/kJ), W_s is compressor work (in kW), p_{LNG} is the difference between feed and product value (in \$/mol) and F_{LNG} is the production rate (in mol/s). Jensen and Skogestad (2006) describe two "modes" of operation, with different optimization objectives.

- Mode I: When energy is expensive, it is optimal to produce just the amount one is bound to (i.e. by contracts with customers). In this mode, the throughput of natural gas (F_{LNG}) is given, and we want to minimize W_s.
- Mode II: When energy is cheap, it is profitable to produce as much as possible. Then F_{LNG} is a degree of freedom, which we seek to maximize.

Jensen and Skogestad (2006) studied Mode II, whereas we will be focusing on Mode I, and consider F_{LNG} a disturbance.

Table 1
Values of stream variables and pressure drops copied from Jensen and Skogestad (2006).

Variable	Value
Feed flow rate [kmol/h]	$1.517 \cdot 10^4$
Feed pressure [bar]	40.0
Feed temperature [°C]	30.0
Feed mole fraction CH_4	0.897
Feed mole fraction C_2H_6	0.055
Feed mole fraction C_3H_8	0.018
Feed mole fraction C_4H_{10}	0.001
Feed mole fraction N_2	0.029
MR flow rate [kmol/h]	$6.93 \cdot 10^4$
Compressor speed ω [rpm]	1000
MR Condensation temperature [°C]	30.0
Compressor inlet pressure [bar]	4.445
Hot MR temperature at HX outlet [°C]	−157.0
NG temperature at HX outlet [°C]	−157.0
Turbine outlet pressure [bar]	10.29
MR mole fraction CH_4	0.327
MR mole fraction C_2H_6	0.343
MR mole fraction C_3H_8	0.000
MR mole fraction C_4H_{10}	0.233
MR mole fraction N_2	0.097
Condenser ΔP [bar]	0.10
NG ΔP in HX [bar]	5
Hot MR ΔP in HX [bar]	4
Cold MR ΔP in HX [bar]	1
Compressor suction ΔP [bar]	0.3 (nominal)
Turbine suction ΔP [bar]	0.3

Table 2
Differences in key variables between this work and Jensen and Skogestad (2006).

Variable	This work	Jensen's work
W_s [MW]	119	120
Compressor outlet pressure [bar]	30.2	30.0
Compressor efficiency η	81.8	82.8
ΔT_{sup} [°C]	5.1	11.3
$\Delta T_{\text{min,Hx}}$ [°C]	1.57	
UA_{NG} [kW/°C]	$9.20 \cdot 10^3$	$8.45 \cdot 10^3$
UA_{MR} [kW/°C]	$4.62 \cdot 10^4$	$5.32 \cdot 10^4$

2.4. Degrees of freedom and disturbances

The process has got a total of ten manipulated variables. These are:

1. Natural gas feed flow rate
2. Mixed refrigerant flow rate

3–5. Mixed refrigerant pressures (high, intermediate and low)

6. Cooling water flow in MR condenser

7–10. .Four molar fractions in MR (since we have five components)

As stated above, we will here consider the case where the natural gas feed flow rate is a *disturbance*, i.e. it is set upstream. Like Jensen and Skogestad (2006), we will also assume that the MR composition cannot be changed during operation. Thus, we have five degrees of freedom left before active constraints are taken into account.

The other disturbance we will consider, besides feed flow rate, is the ambient temperature (i.e. the temperature of the external coolant). The ambient temperature influences directly on the refrigerant pressure. The lower the temperature of the coolant is, the lower we may set the condensation pressure (i.e. the pressure at

[1] For the case study process, when assuming a 1 °C temperature increase for the cooling water, a minimum ΔT of 4 °C in the condenser, and a pressure drop of 1 bar for cooling water, we found a pumping power of 15 kW compared to the 120 MW consumed by the compressor.

the compressor outlet). Like Jensen and Skogestad (2006), we finally assume that maximum cooling is used in the condenser. This means the ambient temperature sets the condensation temperature of the refrigerant directly. This assumption consumes a degree of freedom, bringing us down to four degrees of freedom for optimization.

In a real plant, feed composition will also vary, and it will influence on the work required for liquefaction. Generally, a higher content of NGL components (propane and heavier) will require more cooling, because these components have a higher heat capacity than methane. Since the refrigerant composition cannot be manipulated, the way to compensate for a change in feed composition is to change the refrigerant flow rate. This is the same as for a change in feed flow rate.

2.5. Constraints

The constraints in a liquefaction process are related to the state of the product stream (temperature being the most important, usually there is also a constraint on the content of nitrogen) and to cooling and compression capacity. For a given outlet/inlet pressure ratio, a compressor will have a minimum flow rate it can handle (known as the surge flow rate) and a maximum flow rate (known as the stonewall flow rate). Jensen and Skogestad (2006) consider the surge limit, but not the stonewall limit. Instead, they consider a maximum available compressor work.

Here, we will consider the following constraints:

1. Exit temperature of natural gas leaving the heat exchanger ($T_{NG,out} \leq -157$ °C). *This constraint is always active*.
2. Superheating of refrigerant leaving the heat exchanger ($\Delta T_{sup} \geq 5$ °C).
3. Like Jensen and Skogestad (2006), we consider compressor surge as a constraint ($\Delta M_{surge} \geq 0$).
4. Maximum compressor work is 132 MW. We set it 10% higher than in Jensen and Skogestad (2006) to be able to study the effect of higher feed rates than the nominal one. Since the results from Jensen and Skogestad (2006) give the maximum processing rate, using the exactly same data would not allow us to study higher feed rates.
5. The stream leaving the turbine must be liquid only ($\Delta P_{sat} \geq 0$). In Jensen and Skogestad (2006), this constraint is handled by adding a choke valve and a liquid receiver directly after the turbine (and before the main choke valve). The first choke valve has a fixed pressure drop, and the turbine outlet pressure is indirectly given by the temperature of the refrigerant stream leaving the heat exchanger. Here, we let the turbine outlet pressure be a degree of freedom, and add this constraint.
6. Compressor speed, ω, is limited upwards to 1200 rpm (again, it is set higher than in Jensen and Skogestad (2006) to see how other constraints behave at higher than nominal feed rates).

It is clear that the first constraint will always be active, because it is never optimal to cool the natural gas more than we need to. In this work, this constraint has been implemented by simply specifying this temperature in the Unisim model (in a real process, it would have to be controlled). We are therefore left with *four* degrees of freedom for optimization.

2.6. Nominal optimum of the process

Since there were some discrepancies between the Unisim model used here and the gPROMS model used by Jensen and Skogestad (2006), a re-optimization was carried out. Compressor work (W_s) was minimized, subject to the following constraints listed in Section 2.5 (repeated here for convenience):

1. $T_{NG,out} = -157$ °C
2. $\Delta T_{sup} \geq 5$ °C
3. $\Delta M_{surge} \geq 0$ kmol/s
4. $W_s \leq 132$ MW
5. $\Delta P_{sat} \geq 0$ (no vapour at turbine outlet)
6. $\omega \leq 1200$ rpm

The **fmincon** interior-point algorithm was used. 10 initial points within the bounds were generated, and optimization carried out from each. The optimal values of the optimization variables are shown in Table 3.[2]

Table 4 summarizes the most important variables not included as decision variables.

The following points are worth discussing:

1. ΔP_{sat} is much smaller than in Jensen and Skogestad (2006). This shows that it is optimal to do as much of the expansion as possible in the turbine. This allows for a lower temperature in the cold refrigerant stream, thus giving a larger ΔT at the cold end of the exchanger, and allows us to circulate less refrigerant.
2. ΔM_{surge} is zero (i.e. we operate on the surge limit). This is the same as was found by Jensen and Skogestad (2006). In our case this is to be expected, simply because the surge limit coincides with the flow that, at any given speed, corresponds with maximum efficiency.

Table 3
Optimum at nominal disturbances. Variables listed in bold are added to the variable set to meet equality constraints.

Variable	This work	Jensen's work
MR flow rate [kmol/s]	16.94	18.70
Compressor speed ω [rpm]	1143	1000
Compressor inlet pressure [kPa]	383.2	414.0
Turbine outlet pressure [kPa]	552.5	1029
Compressor inlet T [°C]	15.8	N/A
T_{MR} **at HX outlet** [°C]	−163.9	−157.0
T_{NG} **at HX outlet** [°C]	−157.0	−157.0

Table 4
Other key variables at nominal optimum.

Variable	This work	Jensen's work
Compressor work W_s [MW]	116.4	120.0
ΔT_{sup} [°C]	19.4	11.3
$\Delta T_{min,Hx}$ [°C]	0.7	N/A
Compressor efficiency η	82.1	82.8
ΔM_{surge} [%]	0	0
ΔP_{sat} [kPa]	1.1	20

3. Results

First, one should use process insight to predict which regions must be present, and which constraints will always (or never) be active. The following can be stated even with limited *a priori* knowledge of the process:

1. The temperature of natural gas leaving the heat exchanger will always be at its maximum, as stated above.

[2] This particular solution was found in 5 of the 10 optimization runs. The other 5 runs did not converge to a feasible solution.

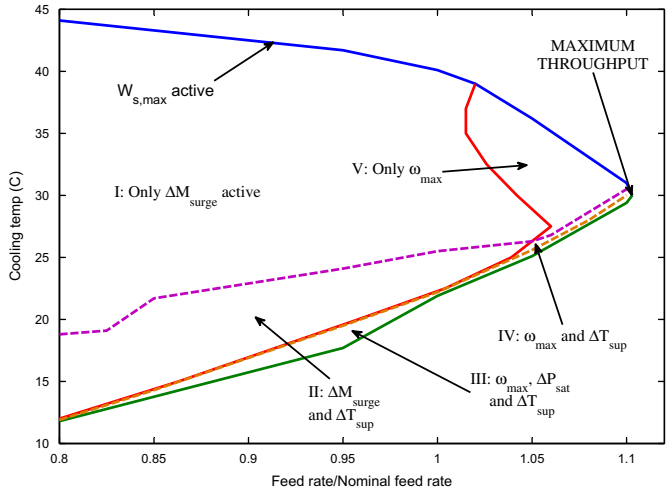

Fig. 2. Active constraint regions for the PRICO process, as function of feed flow rate F and ambient temperature T_{amb}.

2. For a given value of T_{amb}, a maximum throughput (feed flow rate) must exist. This maximum throughput will be low for high values of T_{amb} as the maximum work constraint becomes active.
3. As we lower P_h to exploit the lower T_{amb}, we must reduce compressor speed. This leads to a lower surge limit, which means that the surge margin constraint may become inactive at lower values of T_{amb}.
4. Theoretically, there may be as many as 26 feasible regions: Since each of the five constraints may be either active or inactive, there are $5^2 = 32$ possible combinations. However, only the combinations with three or fewer active constraints are feasible. This means we must subtract the five possible combinations of four active constraints, and the one with five active constraints.
5. Since we have only three degrees of freedom, we can only satisfy three constraints at any time. The maximum possible throughput will coincide with a point where four constraints are active.

First, the feasible region was worked out by starting at the nominal optimum, and optimizing for increasing values of T_{amb} and F until no feasible solution could be found.[3] The constraint curves corresponding to each individual constraint were then found using the interpolation method used in Jacobsen and Skogestad (2011a). The resulting regions are shown in Fig. 2. Notice that the feed rate is given as $F/F_{nominal}$.

When examining Fig. 2, we find that there are five active constraint regions. The active constraints inside each region are summarized in Table 5.

Each curve in Fig. 2 shows where a constraint switches from active to inactive:

1. The blue line, indicating the *maximum* feasible ambient temperature for a given flow rate, gives the upper boundary of the feasible region. Along this line, the maximum constraint on W_s is active.
2. The green line indicates the *minimum* feasible ambient temperature.

[3] This could also have been done by including F as a degree of freedom, and then maximize it at a sufficient number of values for T_{amb}.

Table 5
Active constraints in each region for the PRICO process.

Region number	Active constraint(s)
I	ΔM_{surge}
II	ΔM_{surge}, ΔT_{sup}
III	ω_{max}, ΔP_{sat}, ΔT_{sup}
IV	ω_{max}, ΔT_{sup}
V	ω_{max}

3. The purple dashed line indicates where the superheating constraint (ΔT_{sup}) becomes active.
4. The orange dashed line indicates where the turbine outlet saturation constraint (ΔP_{sat}) becomes active.
5. The red line shows where the maximum speed constraint becomes active (and the surge constraint becomes inactive).

Table 6 gives optimal values for key data at a point in each of the five regions (for Region I, the nominal point from Section 2.6 is given). The numbers shown in bold correspond to constraints that were found to be active to within the specified tolerance.

4. Discussion

4.1. Active constraint regions

Compared to the maximum possible number of regions (26), we find that we have a relatively small number of regions (5). What is of particular interest, is that the constraint curves for ΔM_{surge} and ω_{max} are identical – these two constraints switch along the curve shown in red in Fig. 2. There is no region where both ω_{max} and ΔM_{surge} are active at the same time. This is probably because the surge limit is set to coincide with the flow giving the highest adiabatic efficiency. Consider a given temperature in Region I, where the surge constraint is active. Now assume that the feed F is increased gradually. As long as the active constraints do not change, we may change the refrigerant flow rate proportionally, and at the same time adjust the compressor speed so that we remain at the speed yielding the maximum efficiency. At some point we reach $\omega = \omega_{max}$. A further increase in F must still be followed by an increase in refrigerant flow rate, but the flow rate corresponding to compressor surge is no longer increasing. Thus, ΔM_{surge} cannot remain equal to zero. Fig. 3 shows how these two constraints switch when we go from Region I to Region V.

Table 6
Values for key variables for various values of (F, T_{amb}). Active constraints are shown in bold.

Region	I	II	III	IV	V
T_{amb} [°C]	30.0	18.0	19.3	25.7	30.0
$F/F_{nomical}$	1.00	0.85	0.95	1.05	1.08
MR flow rate [kmol/s]	16.94	14.19	14.91	17.55	18.75
Comp. speed ω [rpm]	1143	1017	**1200**	**1200**	**1200**
Comp. inlet P [kPa]	383.2	323.6	322.4	380.1	408.6
Turb. outlet P [kPa]	552.5	463.5	447.7	538.2	592.7
Comp. inlet T [°C]	15.8	−2.7	−2.8	1.3	6.9
T_{MR} at HX outlet [°C]	−163.9	−167.4	−168.0	−164.4	−162.4
Comp. work W_s [MW]	116.4	86.6	98.8	116.9	127.2
Comp. efficiency η [%]	82.1	82.2	81.9	82.1	82.1
ΔT_{sup} [°C]	19.4	**5.0**	**5.0**	**5.0**	8.8
$\Delta T_{min,Hx}$ [°C]	0.70	0.43	0.25	0.58	0.79
ΔM_{surge} [%]	**0.00**	**0.00**	0.90	0.01	0.01
ΔP_{sat} [kPa]	1.1	1.9	**0.4**	1.2	0.9
$T_{NG,out}$ [°C]	**−157.0**	**−157.0**	**−157.0**	**−157.0**	**−157.0**
Unconstrained DOF	2	1	0	1	2

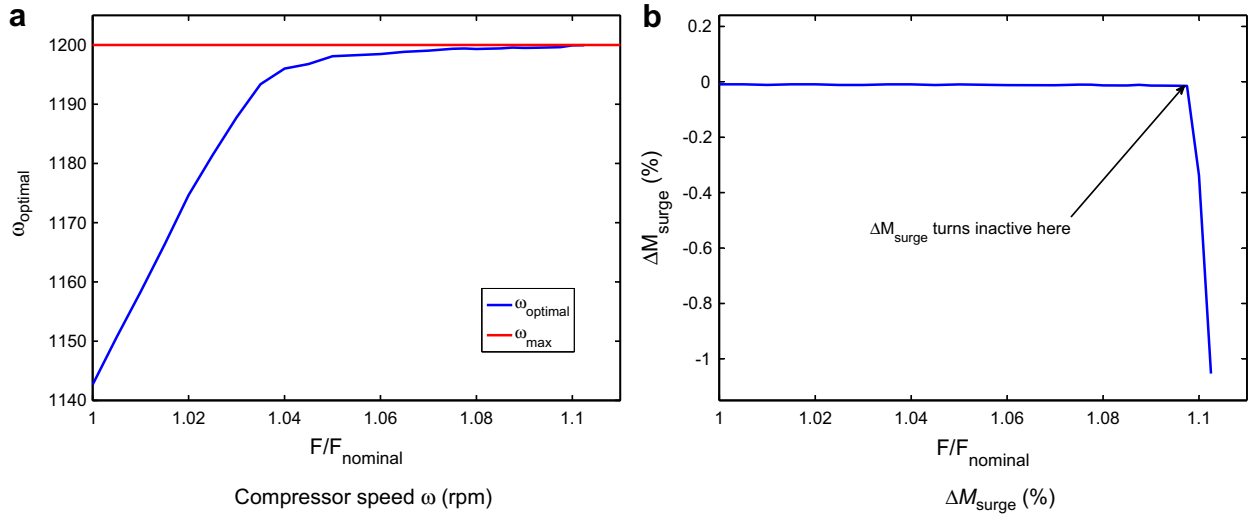

Fig. 3. Plots of optimal compressor speed (ω) and distance to surge (ΔM_{surge}) as function of $F/F_{nominal}$ when going from Region I to Region V.

This also means that two neighbouring regions have the same number of constraints. This is not very common, and usually happens when the two constraints are related to the same unit operation.

The green "minimum" curve shown in Fig. 2 may not be a true minimum. In Region III, there are three active constraints. Along a feasibility limit there should be four; since we have three degrees of freedom, we are able to meet three active constraints. However, when approaching the "minimum" curve, the minimum temperature approach in the heat exchanger becomes so small that it falls within the constraint tolerance, making convergence difficult. What is observed, though, is that within this region compressor work will *increase* with decreasing ambient temperature. This happens because maximum compressor speed is reached, causing a drop in compressor efficiency. Fig. 4 shows how η changes as T_{amb} is gradually reduced from its nominal value of 30 °C to the minimum feasible temperature, at nominal flow rate.

4.2. Issues in optimization

When finding the feasibility limits, quite many optimizations were needed, especially for the lower limit. This might have been avoided if a slightly different form of the optimization problem had been used for this particular task. If feed rate had been included as a degree of freedom, leaving T_{amb} as the only disturbance, the feasibility limit could have been found by maximizing the feed rate, subject to the same constraints as before. The reason why this approach was not used, was that it would have required making alternative versions of nearly all the MATLAB files used.

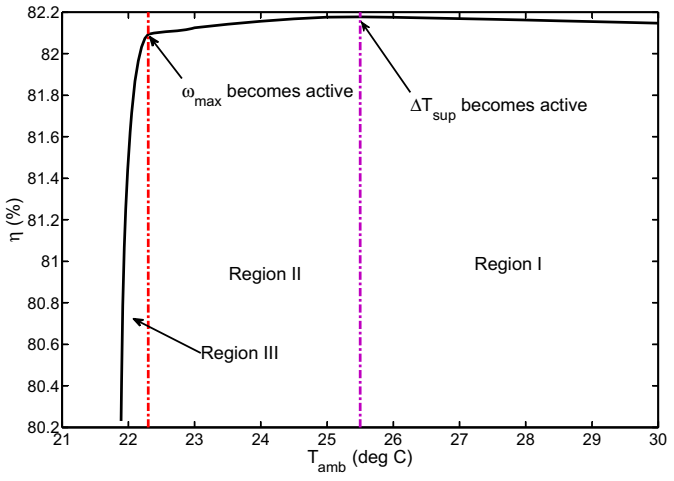

Fig. 4. Compressor efficiency at the optimal solution, as function of ambient temperature T_{amb} for $F = F_{nominal}$.

The **fmincon** solver used in this work, can use two different algorithms: An **active-set** method, and an **interior-point** method (Byrd et al., 2000). The former does not require that bound constraints are satisfied at every intermediate point, whereas the latter does. Because values outside of the specified bounds were likely to cause the flowsheet solver to fail to converge, the interior-point algorithm has been used for all optimizations in this paper. A drawback with this algorithm is that due to its use of slack variables, it may give a solution where a constraint function c is negative and its corresponding Lagrange multiplier λ is positive at the same time. This may introduce some extra uncertainty to the solution of the equation

$$s = c + \lambda \tag{3}$$

which is used to determine the constraint curves.

4.3. Control

For optimal operation, the active constraints should obviously be controlled at all times. In the case studied here, there are five active constraint regions, so theoretically, five different control structures are needed. However, if one control structure is optimal in one region and near-optimal in another, it may be better to use the same control structure, thus simplifying the necessary switching logic. In our case, we see that Regions III and IV are very small, and it could be argued that it is not necessary to include control structures for these, but instead use the same structure as for Regions II and V, respectively.

1. In all regions, $T_{NG,out}$ must be controlled.
2. In Regions I and II, ΔM_{surge} should be controlled, and in the other regions, ω should be at its maximum. Thus it makes sense to use ω to control ΔM_{surge} (possibly via a cascade loop).
3. ΔP_{sat} should be controlled in Region III. However, its optimal value is close to zero in the other regions as well, and it makes sense to control it in all regions.

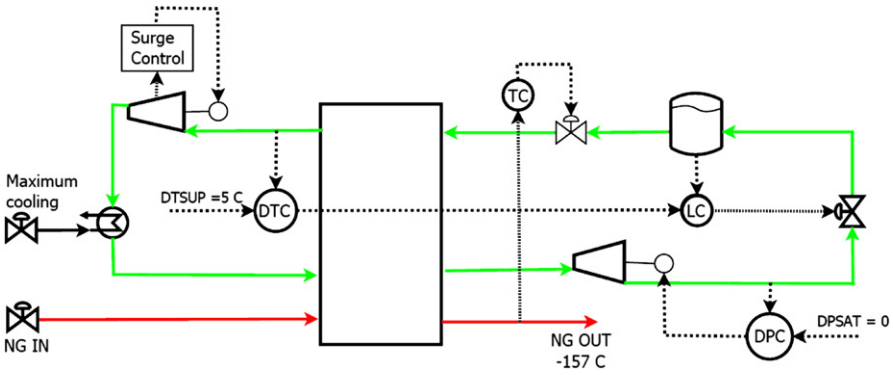

Fig. 5. Suggested control structure for the PRICO process. TC = Temperature controller, LC = level (active charge) controller, DTC = ΔT controller and DPC = ΔP controller.

4. ΔT_{sup} must be controlled in Regions II, III and IV. However, in Regions I and V it seems like a bad choice, as its optimal value is far from the constraint value. An alternative variable to keep constant could be the active charge, as discussed below.

One of the degrees of freedom in the process is related to the *active charge* of the plant (Jensen, 2008). In order to be able to use this degree of freedom, we must be able to change the active charge. This may be done if we introduce an extra valve and a liquid receiver after the turbine, like in Jensen and Skogestad (2006). If this is included, the active charge can be adjusted by changing the set point for the level in this receiver. Alternatively, the active charge itself may be used as a controlled variable.

By introducing this, we suggest the following control structure, illustrated in Fig. 5.

1. The natural gas outlet temperature from the main heat exchanger is controlled at −157 °C, using the choke valve between the turbine and the main heat exchanger.
2. Compressor speed ω is used to keep $\Delta M_{surge} = 0$.
3. Turbine speed is used to control $\Delta P_{sat} = 0$.
4. In Regions II, III and IV, the active charge is used to control $\Delta T_{sup} = 5$ °C. In Regions I and V this controller is switched off, and the active charge controller can instead operate with a constant, default set point.

4.4. Applicability to other liquefaction processes

The PRICO process is a very simple process compared to many that are in use in the industry today. However, several points made in this paper are valid for all kinds of refrigeration processes. The compressor characteristic sets both maximum and minimum limits to the ambient conditions the process can handle. If the assumed location of the surge limit (i.e. near the peak efficiency) is reasonable, the results found here are probably applicable to most liquefaction processes.

A complicating factor is that many plants integrate NGL recovery in the liquefaction train. This will introduce additional constraints in the optimization problem. It will also make operation more dependent on feed composition.

5. Conclusions

This paper discusses active constraints for the PRICO process for liquefaction of natural gas.

We find that for increasing feed flow rate, the acceptable range of ambient temperatures becomes narrower in both ends: As feed flow rate is increased, the maximum acceptable T_{amb} goes down, and the minimum acceptable T_{amb} goes up.

We find five regions with different sets of active constraints inside the feasible area. Based on these results, we propose to control the compressor surge margin and turbine saturation margin at zero in all regions. In Regions I and V we have one additional unconstrained degree of freedom, which should be used to control an additional self-optimizing variable.

The model/problem formulation with the extra equality constraints was found to be efficient, achieving convergence in a majority of the calls to the optimization routine.

References

Aspelund, A., Gundersen, T., Myklebust, J., Novak, M., Tomasgard, A., 2010. An optimization-simulation model for a simple LNG process. Computers & Chemical Engineering 34 (10), 1606–1617.

Byrd, R.H., Gilbert, J.C., Nocedal, J., 2000. A trust region method based on interior point techniques for nonlinear programming. Mathematical Programming 89, 149–185. http://dx.doi.org/10.1007/PL00011391.

Chelouah, R., Siarry, P., 2005. A hybrid method combining continuous Tabu search and Nelder–Mead simplex algorithms for the global optimization of multiminima functions. European Journal of Operational Research 161 (3), 636–654.

Jacobsen, M., Skogestad, S., 2011a. Active constraint regions for optimal operation of chemical processes. Industrial & Engineering Chemistry Research 50 (19), 11226–11236.

Jacobsen, M., Skogestad, S., 2011b. Optimization of LNG plants – challenges and strategies. In: Proceedings of the 21st European Symposium on Computer Aided Process Engineering, Chalkidiki, Greece, May 29–June 1, 2011, pp. 1854–1858.

Jensen, J.B., Skogestad, S., 2006. Optimal operation of a simple LNG process. In: Proceedings Adchem 2006. IFAC, Gramado, Brazil, pp. 241–247.

Jensen, J., 2008. Optimal Operation of Cyclic Processes – Application to LNG Processes. Ph.D. thesis, NTNU.

Lee, G., Smith, R., Zhu, X., 2002. Optimal synthesis of mixed-refrigerant systems for low-temperature processes. Industrial & Engineering Chemistry Research 41 (20), 5016–5028.

Michelsen, F.A., Lund, B.F., Halvorsen, I.J., 2010. Selection of optimal, controlled variables for the TEALARC LNG process. Industrial & Engineering Chemistry Research 49 (18), 8624–8632.

Nogal, F., Kim, J., Perry, S., Smith, R., 2008. Optimal design of mixed refrigerant cycles. Industrial & Engineering Chemistry Research 47 (22), 8724–8740.

Pillarella, M., Bronfenbrenner, J., Liu, Y., Roberts, M., 2005. Large LNG trains: developing the optimal process cycle. In: GasTech 2005, Bilbao, Spain.

Price, B., Mortko, R., 1996. PRICO – a simple, flexible proven approach to natural gas liquefaction. In: GASTECH, LNG, Natural Gas, LPG International Conference, Vienna.

Singh, A., Hovd, M., Kariwala, V., 2008. Control variables selection for liquefied natural gas plant. In: Presented at the 17th IFAC World Congress, Seoul, South Korea, Jul 6–11, 2008.